Avrupa Bilim ve Teknoloji Dergisi
Sayı 35, S. 54-61, Nisan 2022

Araştırma Makalesi

www.ejosat.com ISSN:2148-2683

European Journal of Science and Technology
No. 35, pp. 54-61, April 2022

Research Article

Microstructural and Mechanical Properties of AA7075 Al Alloys Produced via Mechanical Alloying Process

Kemal Doğan[1*], Mustafa Acarer[2], Yasin R. Eker[3], Emin Salur[4]

[1*] Harran University Research Center for Science and Technology , Osmanbey Campus, Şanlıurfa, Turkey, (ORCID: 0000-0002-9770-8069), kdogan@harran.edu.tr
[2] Selçuk University, Faculty of Technology, Department of Metallurgical and Materials Engineering, Konya, Turkey, (ORCID: 0000-0003-2876-4881), macarer@selcuk.edu.tr
[3] Necmettin Erbakan University, Faculty of Engineering, Department of Metallurgical and Materials Engineering, Konya, Turkey, (ORCID: 0000-0001-7395-4364), yeker@erbakan.edu.tr
[4]Selçuk University, Faculty of Technology, Department of Metallurgical and Materials Engineering, Konya, Turkey, (ORCID: 0000-0003-0984-3496), esalur@selcuk.edu.tr

(First received 24 December 2021 and in final form 22 March 2022)

(**DOI:** 10.31590/ejosat.1041205)

ATIF/REFERENCE: Doğan, K., Acarer, M., Eker, Y. R. & Salur, E. (2022). Microstructural and Mechanical Properties of AA7075 Al Alloys Produced via Mechanical Alloying Process. *European Journal of Science and Technology*, (35), 54-61.

Abstract

In this study, it is aimed to produce AA7075 materials by mechanical alloying and sintering methods. Besides, the main purpose of this study is to investigate the effect of different ball milling times on the powder and sintered samples. The milled powders and sintered samples were thoroughly investigated by different characterization techniques. Initially, AA7075 alloy powders were milled by planetary high-energy ball milling device with different milling times. While the initial particle size of commercial grade AA7075 powders were calculated 46 µm, the average particle size of the 8 hours milled powders measured as 22 µm. The effect of different milling times (i.e., 0.5, 1, 2, 4 and 8 hours) on the morphological properties of AA7075 milled powders were investigated by scanning electron microscopy (SEM) and particle size analyses. In addition, X-ray powder diffractometry (XRD) was performed to observe the differences in the crystallographic properties of the milled powders. After the powder preparation and characterization stages, in order to determine the effect of the different phases of milling process on the mechanical properties of the produced AA 7075 samples, these milled powders were consolidated via cold press followed by sintering process. According to experimental outcomes, it was observed that when the milling time reached the final stage (8 hours), the relative density of bulk AA7075 decreased by 7%, in contrast the hardness increased by 130% as compared to pure AA7075 sample fabricated by same producing history.

Keywords: AA7075, Ball Milling, Microstructure, Mechanical Properties.

Mekanik Alaşımlama Yöntemi ile Üretilen AA7075 Al Alaşımlarının Mikroyapısal ve Mekanik Özellikleri

Öz

Bu çalışmada, mekanik alaşımlama ve sinterleme yöntemleri ile AA7075 malzemelerinin üretilmesi amaçlanmıştır. Ayrıca, bu çalışmanın temel amacı, farklı bilyeli öğütme sürelerinin toz ve sinterlenmiş numuneler üzerindeki etkisini araştırmaktır. Öğütülmüş tozlar ve sinterlenmiş numuneler, farklı karakterizasyon teknikleri ile kapsamlı bir şekilde incelenmiştir. Başlangıçta, hazır olarak temin edilen AA7075 alaşım tozu, farklı öğütme sürelerinde gezegensel yüksek enerjili bilyeli öğütme cihazı ile öğütülmüştür. Ticari kalite AA7075 tozların başlangıç partikül boyutu 46 µm olarak hesaplanırken, 8 saatlik öğütülmüş tozların ortalama partikül boyutu 22 µm olarak ölçülmüştür. Öğütülmüş AA7075 alaşım tozların morfolojik özellikleri üzerindeki farklı öğütme sürelerinin (yani 0,5, 1, 2, 4 ve 8 saat) etkisi, taramalı elektron mikroskobu (SEM) analizi ve partikül boyut analizleri ile araştırılmıştır. Ek olarak, öğütülmüş tozların kristalografik özelliklerindeki farklılıkları gözlemlemek için X-ışını toz kırınımı (XRD) yapılmıştır. Toz hazırlama ve karakterizasyon aşamalarından sonra, üretilen AA7075 numunelerinin mekanik özelliklerine öğütme işleminin farklı aşamalarının etkisini belirlemek amacıyla, öğütülen bu tozlar soğuk pres ve ardından sinterleme işlemi ile konsolide edilmiştir. Deneysel sonuçlara göre, öğütme süresi son aşamaya (8 saat) ulaştığında, sinterlenmiş AA7075'in bağıl yoğunluğunun %7 azaldığı, buna karşın aynı üretim geçmişi ile üretilen saf AA7075 numunesine göre sertliğin %130 arttığı gözlemlenmiştir.

Anahtar Kelimeler: AA7075, Bilyeli Öğütme, Mikroyapı, Mekanik Özellikler.

[*] Corresponding Author: kdogan@harran.edu.tr

1. Introduction

Today, technological developments have gained momentum due to improvement in new materials with different superior properties (Aslan et al., 2021; Şavklıyıldız & Demir, 2021). The importance of metal-based materials with desired properties plays a vital role in various industrial applications (Güneş et al., 2021; Usca et al., 2021). In this context, different metals and its alloys have received remarkable attention by diverse researchers (Usca, et al., 2021). Among wide range of alloys, aluminum-based alloys are extensively preferred in various industrial area such as aircraft, maritime, automobile, and aviation due to their low specific gravity and high specific strength, excellent thermal conductivity, easy machining, and their low costs (Salur et al., 2021). There are several types of Al alloys classified by their alloying elements. One of the most important types of Al alloys is 7xxx series. The 7xxx alloy system is aluminum alloys with the main alloying element Zn and the most commonly used minor alloying elements Mg and Cu (Salur et al., 2021). These Al alloys are generally used for aerospace and transportation applications due to their high strength and heat treatable properties. The strengths of these alloys, which are used in aircraft body and wing construction in the aviation industry, are increased by aging (precipitate hardening) heat treatments. Among the 7XXX series aluminum alloys, the AA7075 alloy stands out as it has the highest strength (Şavklıyıldız, 2021). Powder metallurgy process is widely used in the production of Al alloys. Materials with desired properties that cannot be obtained with conventional metalworking processes can be produced by PM method (Salur et al., 2019). Moreover, the PM method is characterized by great flexibility in material selection and design. The PM route is currently widely used to produce high strength and/or creep resistant Al alloys with properties beyond conventional metallurgical levels. The best sample for such applications results from a powder with a fine and supersaturated microstructure or a dense dispersion of fine reinforcing particles that resist coarsening and dissolution (Salur et al., 2021). Such microstructures are generally obtained by rapid solidification, mechanical milling, and mechanical alloying. Rapid solidification processing (RSP) increases solubility and reduces grain size. Further microstructural improvement can be achieved by mechanical alloying/ball milling of rapidly solidifying powder (Zebarjad & Sajjadi, 2006). At the same time, mechanical alloying can increase solid solubility compared to RSP. There are two different terms that refer to the processing of powder particles in high-energy ball mills (Basariya et al., 2014). Mechanical alloying is used for processes in which different powder mixtures are milled together. The aim is to obtain a homogeneous alloy through material transfer (Tekin et al., 2021). The method used for milling pre-alloyed powders where material transfer is not the primary goal is called mechanical milling. Mechanical milling is a widely used PM method developed to produce dispersion-enhanced alloys as a result of particle refining of powders and homogeneous dispersion of fine second phase particles (Salur et al., 2021).

Various studies (Abu-Oqail et al., 2019; Nazik et al., 2016; Shkodich et al., 2014; Varol & Ozsahin, 2019; Xu et al., 2017) have been conducted previously to investigate the effect of ball milling process on the structural evolution of different metals and its alloys. While different properties of Al alloys were investigated thoroughly in the context of the powder metallurgy route, the effect of ball milling method on the overall properties of AA7075 Al alloys seem to have received only cursory attention in the open literature. However, it is well known that the production route provides significant changes in the end product properties. Hence, the main purpose of this study is to examine the influence of the different ball milling times on the microstructural and mechanical characteristics of AA7075 alloys produced by cold pressing within the framework process-properties correlation.

2. Material and Method

In this study, commercial aluminum alloy (AA7075) powders were used for bulk material production. The initial AA7075 powders were supplied by Nanografi, Co. Ltd. Company, Ankara. The average particle sizes of commercially available AA7075 powders measured as 38 μm. The chemical composition of the as-received AA 7075 powders was given in Table 1. Figure 1 shows the SEM images of as-received AA7075 powders (SEM EVO LS10). AA7075 powders were milled by a RETSCH-PM 200 high energy planetary ball milling device for 0.5, 1, 2, 4 and 8 hours, respectively, at 400 rpm under the air atmosphere. The ball-to-powder (BPR) ratio was chosen as 10:1 and 10 mm diameter tungsten carbide (WC) balls were used for milling process. A wt. 2% methanol was used as process control agent (PCA). To avoid overheating and cold welding, the powders were milled for 10 minutes and rested for 5 minutes during all milling periods. The changes in the morphologies of the milled powders were analyzed using by scanning electron microscope (SEM, EVO LS10) instrument. The average particle size (APS) of the milled powders was calculated with the particle size analyzer (Mastersizer 2000). A Rigaku ZSX Primus-II XRD model X-ray diffractometer was used to determine the changes in the crystallographical structures of the milled powders. After the milled powders characterization, the densification of these powders was accomplished by cold pressing followed by sintering process. The cold pressing process was applied at a pressure of 450 MPa. After compaction of milled AA7075 powders at different milling times were sintered for 2 hours at 520 ^{o}C under argon atmosphere in a Protherm tube furnace. During sintering process, the heating rate was settled as 10 ^{o}C/min, and the process was finished by 5 oC/min cooling rate to ambient temperature. The sintering steps was shown in Figure 2. The sintering parameters were selected by literature review (Mobasherpour et al., 2013), our previous investigations (Doğan et al., 2022) and prior knowledge assessment. The Brinell-hardness of sintered bulk samples were measured by a "Digirock-Lc-Rbov″ tester under 62.5 kg load with a using 2.5 mm diameter ball. To calculate the theoretical density of the sample, rule of mixtures was employed, and experimental density values of the sintered sample were determined via the "Precisa XB 220A" precise scale. To supply high preciseness and reproducibility in the measured data, three samples were produced by same preparing history. Plus, at least five measurements were made on each different set and the arithmetic average of measured values was reported with their standard deviation values to produce accurate statistical sample. The microstructural changes of the samples were monitored using same SEM instrument.

Table 1. Chemical composition of as-received AA7075 powders

Elements	Zn	Mg	Cu	Fe	Si	Mn	Al
wt. (%)	4.8	2.9	1.8	0.22	0.15	0.05	~90

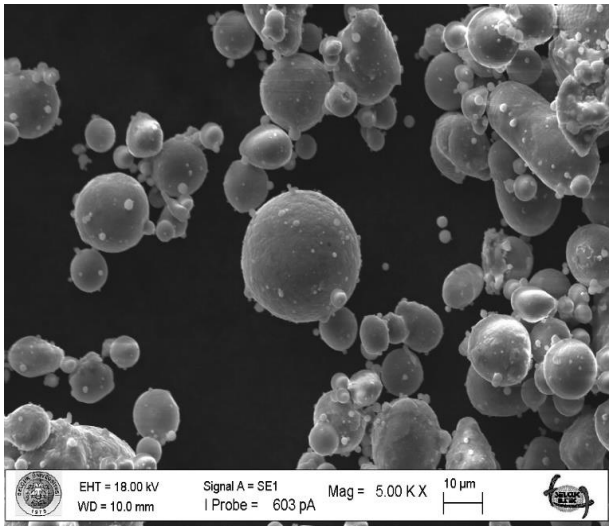

Figure 1. SEM images of as-received AA7075 powders

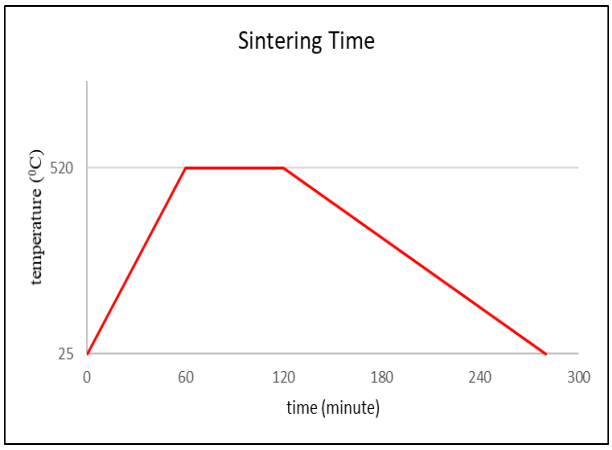

Figure 2. Schematic graph of sintering procedure

3. Results and Discussion

3.1. Powder Characterization

Figure 3 illustrates the SEM images showing morphology of the milled powders for different milling times. In addition, Figure 4 shows the average particle size of the as-received and milled AA7075 powders. Initial AA7075 powders have spherical morphology and about 46 µm in particle size (See Figure 4), as earlier described in Figure 1. In the early stage of the milling (0.5 h), the average particle size (APS) of the powders was decreased to 38 µm due to highly effective PCA. As the milling time increased up to 1 hour, the APS was strikingly increased because of flattened or flake-like pieces, as seen in both Figure 3 and Figure 4. The APS of these powders was measured as 58 µm (See Figure 4). Further milling process up to 8 hours, the flattened AA 7075 powder (Figure 3c and 3d), which was mostly flake in shape and about 60 µm in size, became fractured substantially with decreased due to the severe plastic deformation mechanism triggered by impact forces of powder-ball-jar. In the final stage of milling process (8 hours), the APS value calculated as 22 µm, which is achieved the minimum level of APS, as seen in Figure 4. As described in both Figure 3 and Figure 4, the highest aspect ratio, meaning the ratio between a greatest and smallest dimension of particle sizes, was achieved at 1 hour of milling. The main reason for this situation is the ductile Al powders remaining between the balls is exposed to a micro-rolling effect due to dominant plastic deformation and PCA effect (Suryanarayana, 2001). However, the effect of PCA was gradually faded out in milling system and it resulted in powders subjected to severe fracture mechanism and resultant reduction in particle size. As a consequence, at the end of the milling, there was more than 50% reduction in particle size compared to the initial form (see Figure 4) and randomly fragmented irregular particles were formed as shown in Figure 3

Figure 5a shows the X-ray diffraction curves of the as-received and milled AA7075 powders. The main reflections of the as-received powders were also observed in milled powders. A closer examination at main X-ray curve of the AA7075 powders (Figure 5b), it was observed peak shift towards to high angle as the milling time extended. One reason that of this situation can be originated from stress accumulation on the main lattice structure induced by well-known ball milling effect due to severe plastic deformation under the rigid and tiny balls and their shear forces (Doğan et al., 2022). Such an accumulation on the lattice resulted in increased lattice strain and dislocation density and resultant increment in powder hardness. On the other hand, this observation could be resulted from various parameters such as compositional fluctuations, structural impurities, distribution of reinforcements, stacking faults, and other metallurgical defects (Biçer et al., 2020).

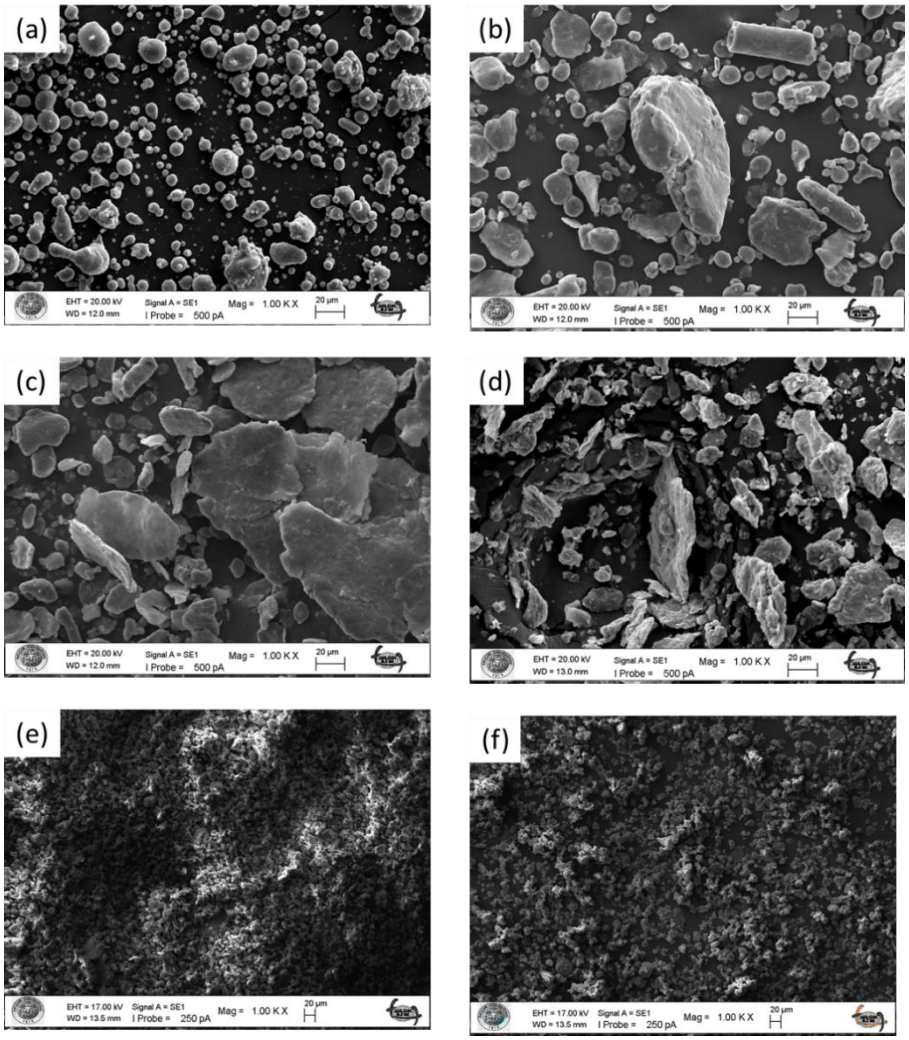

Figure 3. SEM images of the (a) as-received, (b) 0.5h, (c) 1h, (d) 2h, (e) 4h and (f) 8h milled AA7075 powders

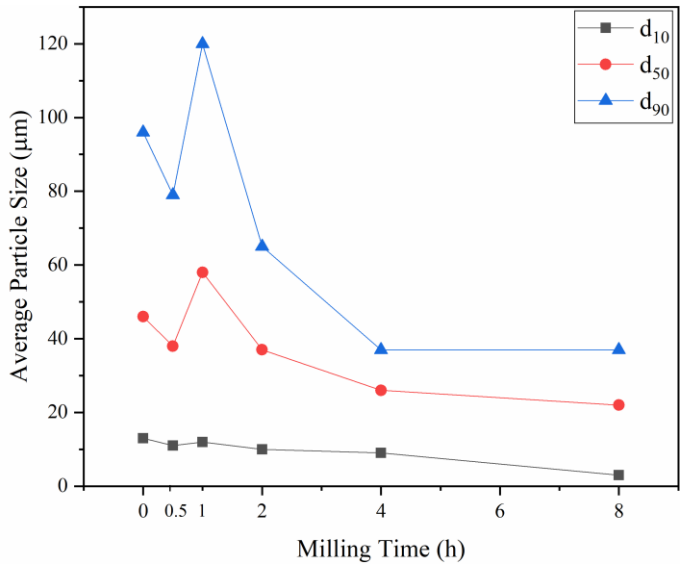

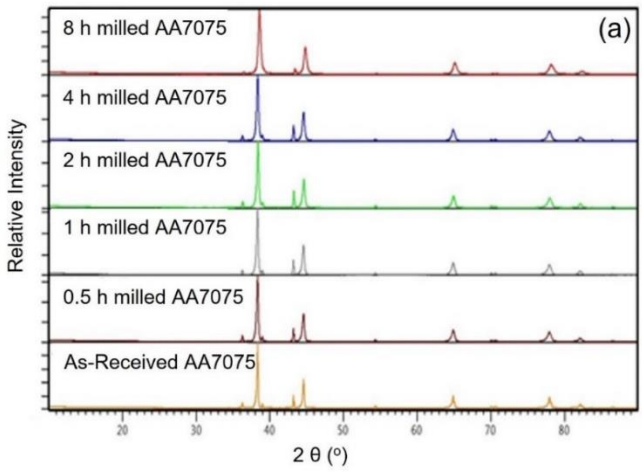

Figure 4. The variation on the average particle size as a function of ball milling time

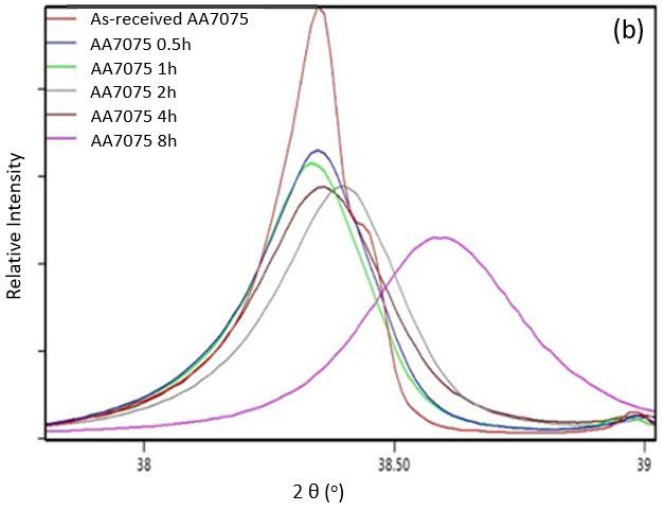

Figure 5. (a) X-ray diffraction curves of as-received and milled AA7075 powders with different milling time and (b) A closer examination on the main reflection peak showing peak shift

3.2. Bulk Material Characterization

Initial particle size, its distribution and particle morphology of each powder directly or indirectly influence the final microstructure of sintered specimens. In this regard, detailed powder characterization is highly vital point to determine the performance of final product. Figure 6 shows the SEM images of consolidated AA7075 Al alloys at different milling times. Considering Figure 3 and Figure 6, it was observed that there is no discernible grain growth in any samples due to sintering process. Figure 6a illustrates the SEM image of sintered as-received AA7075 alloy with a spherical shape with an average grain size of ~ 45 µm. After 0.5 hour of milling, some of the spherical grains transformed into the flattened grains, with the greater part remains in spherical shape (see Figure 6b). Spherical shapes were almost completely turned into flake-like grains along with irregular fractured smaller particles, after 1 hour of milling (See Figure 6c). Similar observations were also reported by some authors who conducting study on the ball milling of different Al-based alloys (Chen et al., 2015; Xu et al., 2017).

Figure 7 shows the experimental density of the sintered samples. As seen in density results, the best packing property was attained at 1 hour of milling stage due to beneficial combination of desired particle size ranges and morphologies, as earlier described in Figure 6c. This phenomenon led to satisfying structural integrity in the material system, and the density of the sample was reached to its maximum level. As the milling time increase up to 8 hours, it was observed that the flake-like grains turned into randomly fractured irregular shapes due to the initially milled particles and repetitive impact of the powder-ball-jar, as presented in Figure 6c-f. Naturally, the average grain size systematically decreased, which shows good agreement with the results of the powder SEM analysis (see Figure 3 and 4).

As illustrated in Figure 8, the Brinell hardness of sintered AA7075 Al alloy increased with prolonging milling time. The sample produced with 8 hours milled powders exhibited 2 times harder than the pure AA7075 sample produced by as-received powders. Severe plastic deformation mechanism on the powder particles can be one issue in that the ball milled powders show improved hardness than traditional deformation mechanisms. These powders subject to the work hardening effect due to increased milling time, which leads to an increased powder hardness. Such an increment in hardness of the particles can be originated from different factors. Increased lattice strain due to increased dislocation density during milling operation is the main factor (Yoo et al., 2013). Besides, decreased grain size is another crucial parameter for enhanced hardness according to the Hall-Patch equation, which defines the correlation between the hardness or strength of polycrystalline materials and the grain size. The existence of the intense dislocation density in the structure accelerates the finer grain formation and it supplies grain refinement with different sub-grains throughout the microstructure (Kang et al., 2018). The different arrangement of neighboring sub-grains and the high lattice distortion at the locality of grain boundaries hinder dislocation movement in the certain shear plane and accompanying hardening the samples. In this regard, aforementioned concurrent parameters are beneficial for increasing hardness of the samples.

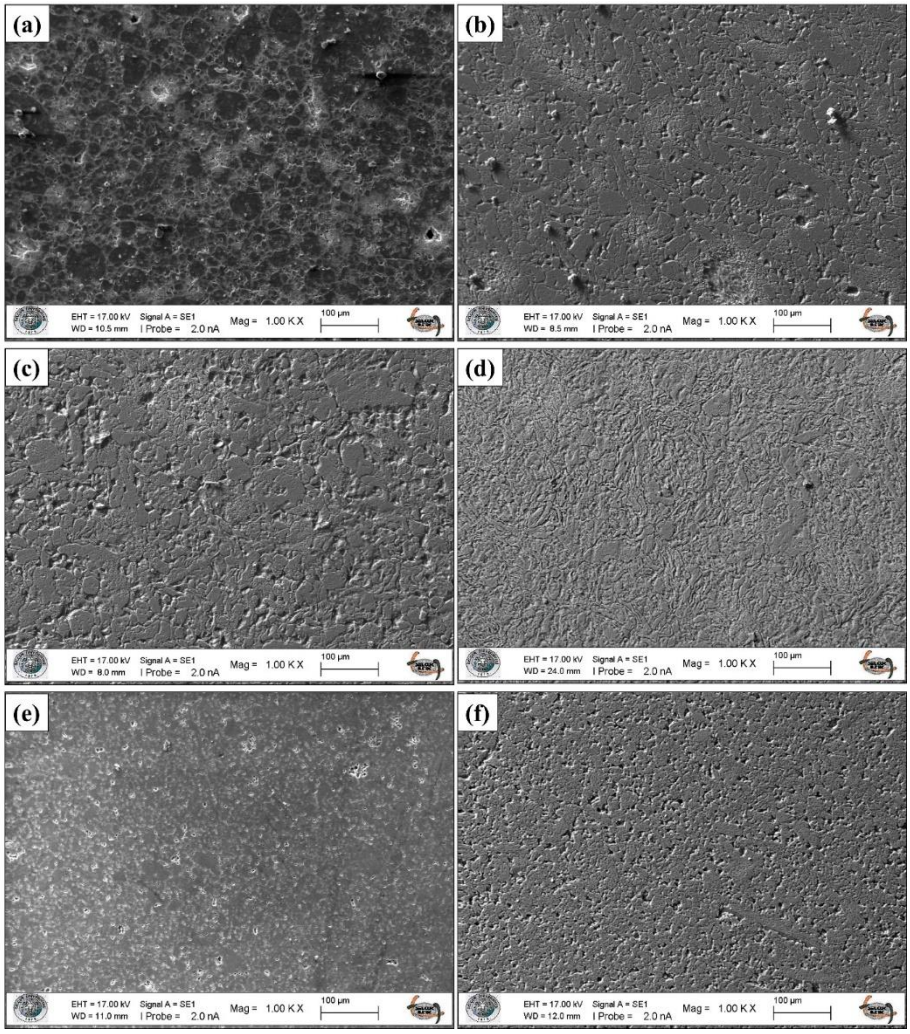

Figure 6. SEM images of sintered samples produced from (a) as-received, (b) 0.5h, (c) 1h, (d) 2h, (e) 4h, and (f) 8h milled powders

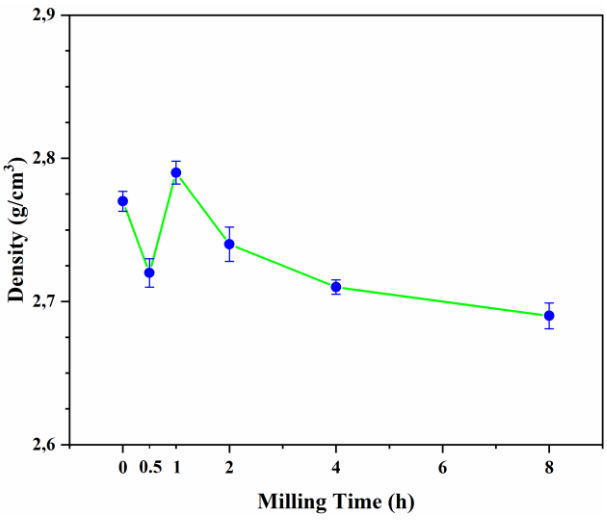

Figure 7. The changes in experimental density of sintered AA7075 Al alloy with different milling times

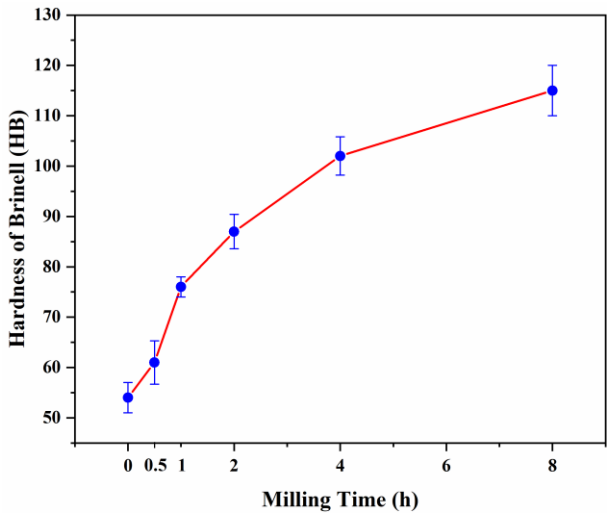

Figure 8. The Brinell hardness of the sintered AA7075 Al alloy with respect to different milling times

4. Conclusions and Recommendations

In this study, the influence of different ball milling times (i.e., 0.5, 1, 2, 4, and 8 hours) on the microstructural, crystallographical, and mechanical properties of the AA7075 Al alloy system were experimentally examined within the framework of plastic deformation mechanism and via ball milling

process. Firstly, the effect of ball milling time on the microstructural evolution and crystallographic characteristics of the milled powders was extensively characterized by particle size analysis, SEM and XRD analyses. After the powder characterization, the microstructure and mechanical properties of the sintered bulk samples was analyzed by SEM, density and hardness results. The experimental results of this study can be listed as follows:

1. The average particle size of the AA7075 powders decreased with increasing milling time. While the average particle size of the as-received AA7075 form was calculated as 46 μm, the average particle size of the 8 hours milled powders measured as 22 μm. Such a decrease in particle size resulted from dominant fracture mechanism, and severe powder-ball-jar collisions. Besides, the morphologies of the powders exhibited differences due to randomly fractured pieces. As the milling time increased, the initial spherical shape of powders turned into irregular shapes.

2. After 8 hours of ball-milling time, the corresponding XRD data revealed a decrement in peak intensity with discernible peak broadening. This was mainly attributed to the hindrance of the dislocation mobility throughout the structure.

3. The composite produced by 1 hours milled powders showed enhanced structural integrity with higher density (2.77 gr/cm^3) owing to the particles' optimum packing and sintering ability. The density of this specimen was improved compared to others.

4. A significant increment in Brinell hardness from 54 to 115 HB (~ 130 %) was obtained in the in the final stage of milling. The achieved ~ 130 % increase in hardness was ascribed to decreased particle size, increased lattice strain and dislocation density, which were triggered by gradually activated plastic deformation mechanism under the high impact of tiny and rigid balls with prolonging milling time.

5. Acknowledge

The authors gratefully acknowledge the financial support provided by the Scientific Research Projects Coordination Unit (SRPCU) of Selçuk University for the project (Contract # 20211036). This paper is derived from Kemal DOĞAN's Ph.D. thesis. A small portion of initial experimental results was presented in International Conference on Engineering Technologies, ICENTE'21.

References

Abu-Oqail, A., Wagih, A., Fathy, A., Elkady, O., & Kabeel, A. (2019). Effect of high energy ball milling on strengthening of Cu-ZrO_2 nanocomposites. Ceramics International, 45(5), 5866-5875.

Aslan, A., Salur, E., Düzcükoğlu, H., Şahin, Ö. S., & Ekrem, M. (2021). The effects of harsh aging environments on the properties of neat and MWCNT reinforced epoxy resins. Construction and Building Materials, 272, 121929.

Basariya, M. R., Srivastava, V., & Mukhopadhyay, N. (2014). Microstructural characteristics and mechanical properties of carbon nanotube reinforced aluminum alloy composites produced by ball milling. Materials & Design, 64, 542-549.

Biçer, H., Akdoğan, E. K., Şavklıyıldız, İ., Haines, C., Zhong, Z., & Tsakalakos, T. (2020). Thermal expansion of nano–boron carbide under constant DC electric field: An in situ energy dispersive X-ray diffraction study using a synchrotron probe. Journal of Materials Research, 35(1), 90-97.

Chen, B., Li, S., Imai, H., Jia, L., Umeda, J., Takahashi, M., & Kondoh, K. (2015). Carbon nanotube induced microstructural characteristics in powder metallurgy Al matrix composites and their effects on mechanical and conductive properties. Journal of Alloys and Compounds, 651, 608-615.

Doğan, K., Özgün, M. İ., Sübütay, H., Salur, E., Eker, Y., Kuntoğlu, M., Acarer, M. (2022). Dispersion mechanism-induced variations in microstructural and mechanical behavior of CNT-reinforced aluminum nanocomposites. Archives of Civil and Mechanical Engineering, 22(1), 1-17.

Güneş, A., Salur, E., Aslan, A., Kuntoğlu, M., Giasin, K., Pimenov, D. Y., Şahin, Ö. S. (2021). Towards analysis and optimization for contact zone temperature changes and specific wear rate of metal matrix composite materials produced from recycled waste. Materials, 14(18), 5145.

Mobasherpour, I., Tofigh, A., & Ebrahimi, M. (2013). Effect of nano-size Al_2O_3 reinforcement on the mechanical behavior of synthesis 7075 aluminum alloy composites by mechanical alloying. Materials chemistry and physics, 138(2-3), 535-541.

Nazik, C., Tarakcioglu, N., Ozkaya, S., Erdemir, F., & Canakci, A. (2016). Determination of effect of B_4C content on density and tensile strength of AA7075/B_4C composite produced via powder technology. International Journal of Materials, Mechanics and Manufacturing, 4(4), 251-261.

Salur, E., Acarer, M., & Nazik, C. (2021). Mekanik Alaşımlama Süresinin Toz Metalurjisi ile Üretilen AA7075 Matrisli Nanokompozit Malzemelerinin Sertliklerine Etkisi. Journal of the Institute of Science and Technology, 11(3), 2218-2231.

Salur, E., Acarer, M., & Şavkliyildiz, İ. (2021). Improving mechanical properties of nano-sized TiC particle reinforced AA7075 Al alloy composites produced by ball milling and hot pressing. Materials Today Communications, 27, 102202.

Salur, E., Aslan, A., Kuntoglu, M., Gunes, A., & Sahin, O. S. (2019). Experimental study and analysis of machinability characteristics of metal matrix composites during drilling. Composites Part B: Engineering, 166, 401-413.

Salur, E., Aslan, A., Kuntoğlu, M., & Acarer, M. (2021). Effect of ball milling time on the structural characteristics and mechanical properties of nano-sized Y_2O_3 particle reinforced aluminum matrix composites produced by powder metallurgy route. Advanced Powder Technology, 32(10), 3826-3844.

Salur, E., Nazik, C., Acarer, M., Şavklıyıldız, İ., & Akdoğan, E. K. (2021). Ultrahigh hardness in Y_2O_3 dispersed ferrous multicomponent nanocomposites. Materials Today Communications, 28, 102637.

Shkodich, N., Rogachev, A., Vadchenko, S., Moskovskikh, D., Sachkova, N., Rouvimov, S., & Mukasyan, A. (2014). Bulk Cu–Cr nanocomposites by high-energy ball milling and spark plasma sintering. Journal of alloys and compounds, 617, 39-46.

Suryanarayana, C. (2001). Mechanical alloying and milling. Progress in materials science, 46(1-2), 1-184.

Şavklıyıldız, İ. (2021). In-Situ Strain Measurement on Al7075 Plate by Using High Energy Synchrotron Light Source. Avrupa Bilim ve Teknoloji Dergisi(23), 435-439.

Şavklıyıldız, İ., & Demir, A. (2021). Flash Sintering Effect on PMN-PT Ceramics. El-Cezeri Journal of Science and Engineering, 8(2), 793-799.

Tekin, M., Polat, G., Kalay, Y. E., & Kotan, H. (2021). Grain size stabilization of oxide dispersion strengthened CoCrFeNi-

Y_2O_3 high entropy alloys synthesized by mechanical alloying. Journal of Alloys and Compounds, 887, 161363.

Usca, Ü. A., Uzun, M., Kuntoğlu, M., Sap, E., & Gupta, M. K. (2021). Investigations on tool wear, surface roughness, cutting temperature, and chip formation in machining of Cu-B-CrC composites. The International Journal of Advanced Manufacturing Technology, 116(9), 3011-3025.

Usca, Ü. A., Uzun, M., Kuntoğlu, M., Şap, S., Giasin, K., & Pimenov, D. Y. (2021). Tribological aspects, optimization and analysis of Cu-B-CrC composites fabricated by powder metallurgy. Materials, 14(15), 4217.

Varol, T., & Ozsahin, S. (2019). Artificial neural network analysis of the effect of matrix size and milling time on the properties of flake Al-Cu-Mg alloy particles synthesized by ball milling. Particulate Science and Technology, 37(3), 381-390.

Xu, R., Tan, Z., Xiong, D., Fan, G., Guo, Q., Zhang, J., . . . Zhang, D. (2017). Balanced strength and ductility in CNT/Al composites achieved by flake powder metallurgy via shift-speed ball milling. Composites Part A: Applied Science and Manufacturing, 96, 57-66.

Zebarjad, S. M., & Sajjadi, S. (2006). Microstructure evaluation of Al–Al_2O_3 composite produced by mechanical alloying method. Materials & design, 27(8), 684-688.